10.3. Monitoring radar Z_{DR} calibration using ground clutter

Valery Melnikov[*] and Dusan Zrnic[+]

[*]- The University of Oklahoma, CIMMS, Norman, OK.
[+] - NOAA/OAR National Severe Storms Laboratory, Norman, OK

1. Introduction

To obtain high quality radar data from clouds and precipitation, radars have to be precisely calibrated. The WSR-88D's system specifications establish uncertainty of ±1 dB and ±0.1 dB for reflectivity (Z) and differential reflectivity (Z_{DR}) estimates. The uncertainties depend on the quality of radar hardware and the statistical of returned radar signals. To monitor radar hardware, the WSR-88Ds have built-in equipment and special procedures. Due to variety of factors that affect radar measurements there is no consensus on sufficiency of built-in radar equipment to achieve indicated accuracies. That is why various procedures have been developed to verify radar calibration. Most such procedures are based on remote sensing of scatterers that possess certain characteristics. To calibrate Z and Z_{DR}, signal reflected from a metal sphere has been utilized (e.g., Bringi and Chandrasekar 2001, section 6.3.1; Atlas 2002, Williams et al. 2013). The main problem with this approach is its arrangement complexity that makes it impractical for routine operational application. Moreover, such measurements estimate the system gain at one point in the antenna pattern which may not be at the center of pattern. Moreover weather scatterers are distributed and therefore besides the gain the shape of antenna pattern needs to be known at least within the mainlobe.

A procedure for relative Z calibration for adjacent WSR-88D radars has been developed (Zhang et al. 2011). This procedure is applied when adjacent radars observe the same parts of precipitation. Reflectivity estimates from these radars should be equal. However, bringing reflectivity to the same level does not guarantee the correct absolute Z calibration, which remains one of the major problems in radar meteorology.

Vertical sensing of precipitation is used in some radars to calibrate Z_{DR}. Raindrops appear round in the mean at vertical incidence if there is no strong wind shear that can incline/cant the drops relative to radar beam (Gorgucci et al. 1999). This method is used in the German, French, and Finnish weather radar networks (Frech 2013, Sugier and Tabary 2006, Vaisala 2014) but cannot be applied to the WSR-88Ds because the maximum elevation angle of their antennas is 60^o.

To calibrate Z_{DR} on the WSR-88Ds, built-in equipment and measurement routines have been designed by the manufacturer and three methods are used operationally for calibration verification (Cunnigham et al. 2013). The first is based on measurements of Z_{DR} in drizzle or light rain. Z_{DR} in drizzle should be close to 0 dB. How close it is to 0 dB remains unknown because drizzles can contain a small number of large drops that can bias Z_{DR} high. It is assumed that climatological Z_{DR} values in light rain for a given region have certain values which could verify long time calibration. Z_{DR} in a given rain can deviate from the climatological mean and should be used with caution.

The second method to verify Z_{DR} calibration utilizes measurements from snow/crystal cloud areas. It is assumed that snow aggregates exist just above the melting layer and that their Z_{DR} is about 0.2 dB. The problem with this approach is that characteristics of snow/crystal particles above the melting layer are not precisely known hence applicability of this approach to a given case remains uncertain. Cloud layers with Z_{DR} much larger than 0.2 dB and located just above the melting layer have been observed with the WSR-88Ds.

The third method is based on observations of reflection from clear air. The top of convective boundary layer contains continuum of turbulent eddies including sizes of about 5 cm (half of the radar wavelength) that cause Bragg scatter of S band radiation (Doviak and Zrnic 2006, chapter 11). Due to small eddies' sizes and their chaotic spatial orientations in turbulent air, their Z_{DR} is 0 dB on the average (Melnikov et al. 2011, Hoban et al. 2013). Bragg scatter is easy to observe in cold seasons; in warm months Bragg scatter is often masked by reflections from insects. Nevertheless, operational radar observations show sufficient detectability of Bragg scatter year round

on almost all radar sites (Cunnigham et al. 2013, Hoban et al. 2013, Ice et al. 2014). There are sites located at high altitudes with dry climate (e.g., in Colorado and Utah), where most of the time Bragg scatter is too weak to be routinely observed.

These three WSR-88D's methods use external objects. The first two methods utilize precipitation that makes Z_{DR} calibration "after the fact", i.e., to calibrate Z_{DR}, sufficient amount of data should be collected. The third method (i.e., Bragg scatter) is used in clear air and should be conducted right before a precipitation event and that is not always possible. Stability of the radar system plays a critical role in calibration: a calibrated system should hold constant its parameters for a sufficiently long time or adjust its drift with the built-in equipment. System drifts are monitored on the WSR-88Ds at the end of every volume coverage pattern (VCP). This allows calibrating Z_{DR} with accuracy better than ±0.2 dB on about 60% of systems (Cunningham et al. 2013, R. Lee, personal communication, 2015). No real time corrections to the system Z_{DR} from the above mentioned external target methods have been implemented yet. There is a need to continuously verify Z_{DR} calibration with external scatterers. This is not achievable with the above mentioned methods. Ground clutter is observed always and can be tested as a calibration object. Results of studying ground clutter for monitoring Z_{DR} calibration at S frequency band are presented here.

2. Ground clutter as a radar calibration object

The characteristics of radar signals reflected from the ground have been studied to obtain information on the types of surfaces, vegetation, the wind near the ground/sea and other environmental features (see a historical overviews in Long 1975 and Billingsley 2002). Dual polarization radar technique has increased the quality of remote sensing of the land and sea and is widely used in SAR radars (e.g., Lee and Pottier 2009). Distributions of the power of reflected signal and their temporal and spatial characteristics have been studied intensively (e.g., Billingsley 2002, Kulemin 2003, Lee and Pottier 2009, Curtis 2009) and large amount of data has been obtained at different spectral bands.

The utilization of ground clutter for reflectivity calibration has been studied since 1970s. Rinehart (1978) reported on using reflections from relatively stable point targets (radio towers) to monitor reflectivity calibration. His measurements showed large variations (more than 7 dB) in reflected powers over time. Delrieu et al. (1997) and Pellarin et al. (1999) utilized reflection from mountains to estimate attenuation at X band. Assuming stable reflections from certain mountains, the authors estimated attenuation caused by precipitation located between the radar and mountains. The presented variations in reflectivity from Mount Saint Cyr for dry periods show the day-to-day reflectivity fluctuations of about ±3 dB for a period of 8 months (Delrieu et al. 1997, their Fig. 3). Vukovic et al. (2015) used ground clutter to monitor reflectivity on a C-band weather radar.

High stability of the system Z_{DR} in X-band radar operated in an urban environment was reported by Borovska and Zrnic (2014). X-band radar of the Bonn University was calibrated on Z_{DR} with the vertically looking antenna. Z_{DR} was also measured from ground clutter within distances of 20 km from the radar and in areas with $Z > 50$ dBZ. The median Z and Z_{DR} from ground clutter exhibited high stability during 17 days of the observations: Z_{DR} was within an interval of ±0.12 dB. These authors also presented observations at S band (WSR-88D KOUN) which showed fluctuations in Z_{DR} from ground clutter in an interval of ±0.2 dB over 3.5 days of the observations.

The cited results are promising, but they do not address directly the calibration issues of the WSR-88D. Therefore we explored signal processing to better select stable ground clutter and collected data in various seasons and under various weather conditions.

3. Processing of clutter signals

Characteristics of ground clutter depend on the properties of terrain and the rate of antenna rotation. Radar Doppler spectra from the ground are formed by two types of scatterers. The first consist of the ground, manmade structures, and big tree trunks all of which are stationary and therefore create a narrow Doppler spectrum whose width is proportional to the antenna rotation rate. The second type of scatterers is created by moving vegetation and vehicles, which are responsible for most of the spectrum width. The relative strength of these contributors depends on the surface type, its wetness, season (foliage), and the surface winds (e.g., Billingsley 2002, Kulemin 2003, Curtis 2009). For calibration purposes, the suppression of the second contribution is desirable because it strongly depends upon environmental conditions.

Ground clutter is very variable spatially: the signal power may change by several dB in adjacent range gates along or across the radial. Strong variations in reflected power may occur in a single range gate at moving antenna from pulse-to-pulse due to changes in the number and types of reflected elements. Thus, the signal properties of ground clutter depend on the antenna rotation rate and can change widely.

The polarimetric WSR-88D measures six variables: reflectivity Z, Doppler velocity, spectrum width, differential reflectivity Z_{DR}, differential phase, and correlation coefficient. We analyze herein Z and Z_{DR} which are calculated from received voltages V_h and V_v in the radar channels with horizontally and vertically polarized waves as,

$$P_h = < V_h^* V_h > - N_h,\ P_v = < V_v^* V_v > - N_v, \quad (1)$$

$$Z = C_r + 10\log_{10}(P_h), \quad (2)$$

$$Z_{dr} = P_h / P_v, \quad Z_{DR} = 10\log_{10}(Z_{dr}), \quad (3)$$

where $N_{h,v}$ are the noise powers in the channels, C_r is the radar constant with range normalization included, and angular brackets stand for time averaging. In the above equations, noise can be ignored because strong signal from the ground is analyzed in this study. One of the most important questions in calibration is feasibility of using ground clutter during regular data collection. So the data from standard VCPs were used in this study.

An example of six radar variables collected with the WSR-88D KOUN (Norman, OK) in "clear air" is in Fig.1 to the range of 50 km where the echo from ground clutter is mainly located. The SNR field contains values exceeding 90 dB. The velocity field shows predominant positive values in the north part of the field and mainly negative values in the south part. This velocity pattern demonstrates that radar captured signals from insects/birds that were flying to the north. High Z_{DR} values at the edges of the Z_{DR} field confirm this conclusion. The spectrum width field has small values in areas with strong echoes from the ground and much larger values in areas with atmospheric biota.

To select ground clutter for this study, echoes from biota and moving objects have been filtered out. To do so, the following constraints were applied to radar data.

- Range of observation was from 2 to 30 km, where most of the ground clutter is located on this site.
- SNR threshold was set at 40 dB in both polarimetric channels to filter out biota echoes.
- Parts of the Doppler spectra from an interval ±0.5 m s^{-1} are processed to select echoes from stationary ground targets. Filtering out signals with spectral components beyond this interval suppresses the signal contributions from moving targets (tree/bush branches, moving vehicles, and flying birds) and also rejects signals leaking from strong stationary clutter, i.e., spectral leakage.

To illustrate the latter constraint, Doppler spectra from a single range gate are depicted in Fig. 2 for M = 16 and 64 (PRF = 320 Hz). A strong spectral leakage is seen in the spectra. These spectral skirts can have contributions from moving targets and illustrate the reason for suppressing these spectral parts. The spectral part in an interval of ±0.5 m s^{-1} is selected for further analysis. For M =16, only one spectral component, i.e., DC, is left in the spectra (Fig. 2a), for M=64, three central lines are left in the spectra (Fig. 2b). After suppressing spectral skirts, the selected spectrum is converted to voltages and all signal characteristics are calculated in time domain according to (1) - (3).

Radar images obtained after applying the above constraint and filtering are in Fig. 3 where the data of Fig. 1 were used. One can see that a big portion of biota echoes has been removed from the images. The spectrum width field has values less than 1 m s^{-1} now (compare with Fig. 2). Distributions of Z_{DR} values obtained with the constraints are plotted in Fig. 4.

The right panel in Figs. 4 exhibits a well pronounced peak at a value close to zero. The system Z_{DR} in KOUN at that time was 0.25 dB, i.e., also close to 0 dB. One of the main goals of this study is obtaining stability of Z_{DR} from ground clutter. To assess this stability, variability of Z_{DR} values at the maximum of distribution has been analyzed. To analyzed stability of Z measurements, the mean SNR has been examined.

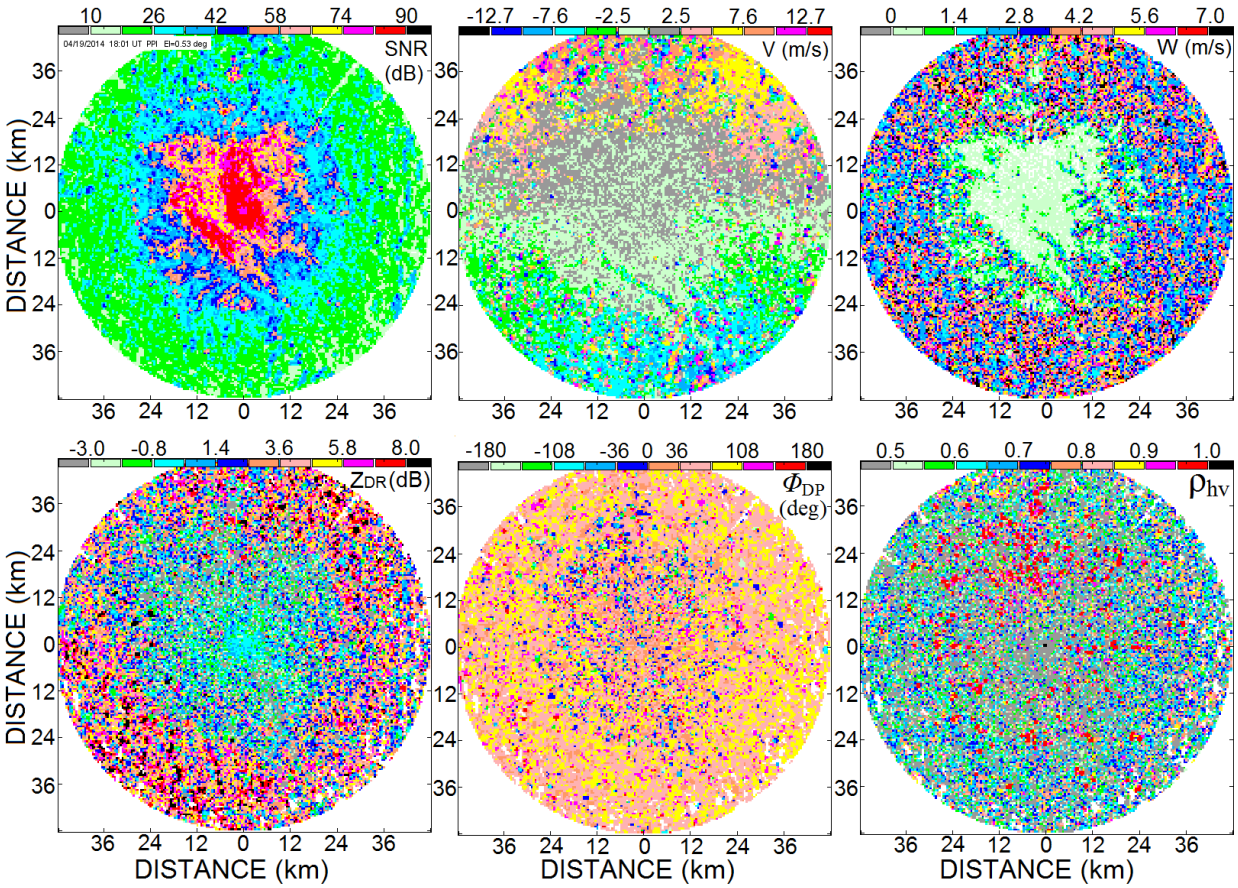

Fig.1. Six radar variables collected with KOUN on April 19, 2014 at 1801 UTC in "clear air". Data are displayed to the range of 50 km.

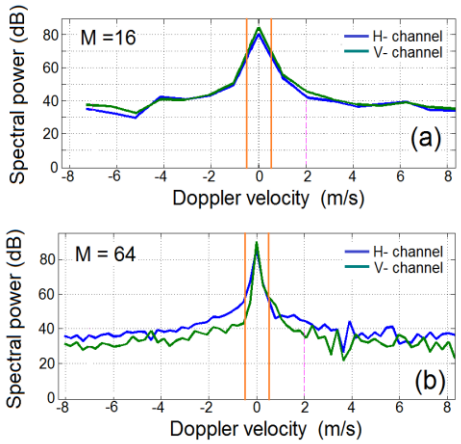

Fig. 2. Doppler spectra in the two polarimetric channels collected with KOUN 06/02/2015 at 0041 UTC at an azimuth of 220^o and a distance of 10 km. The number of samples is (a) M =16 and (b) M = 64. The two brown vertical lines are drawn at velocities ±0.5 m s^{-1}.

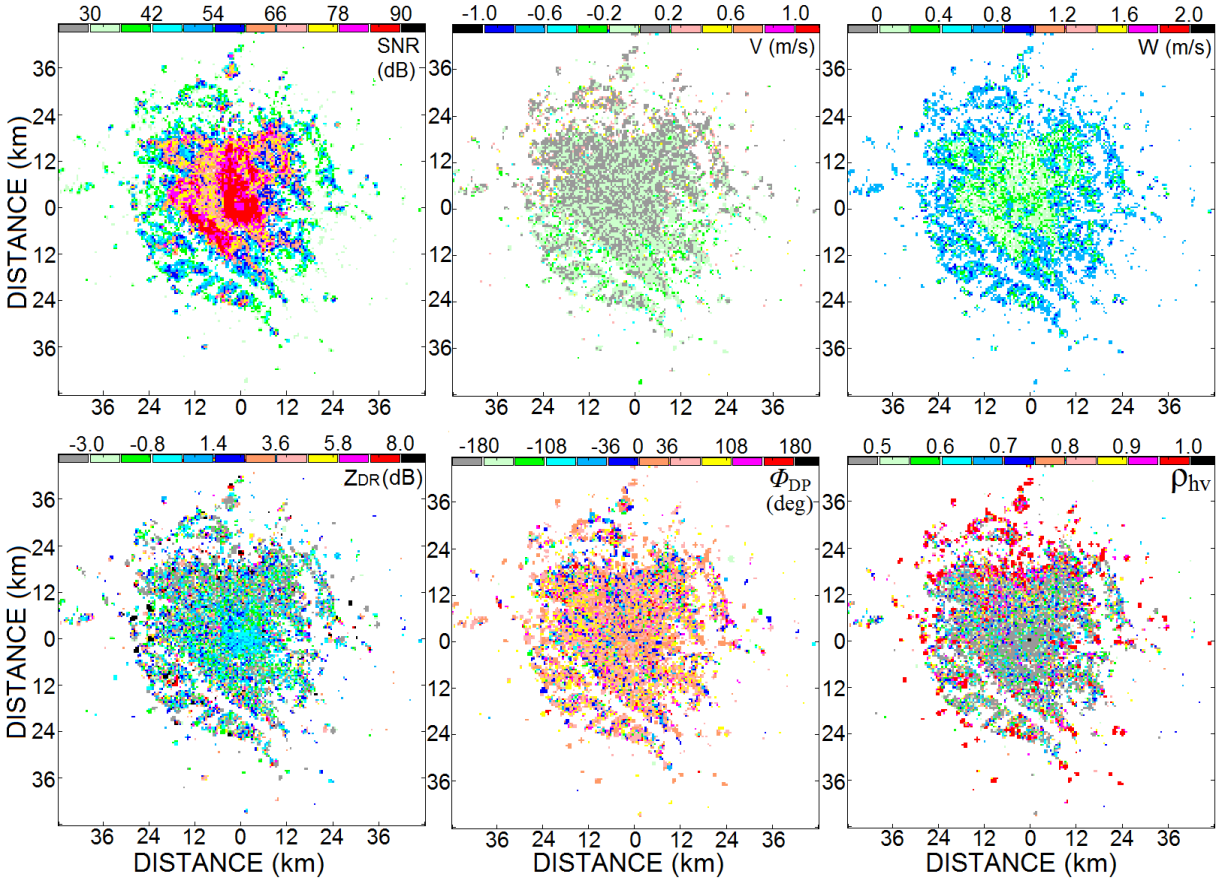

Fig. 3. Fields of six radar moments obtained using constraints a-c in the text with the SNR threshold of 30 dB.

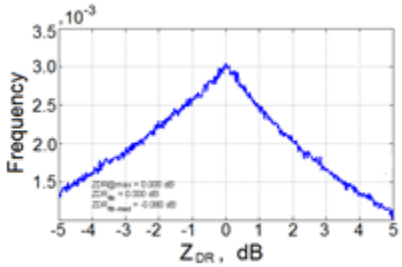

Fig. 4. Distribution of ZDR for data collected on April 19, 2014 from 0000 to 0200 UTC. The total number of data points is 2.17x10^6.

4. Feasibility of reflectivity monitoring

Radar reflectivity Z is calculated from SNR in the horizontal radar channel. In our study, the mean SNR was obtained for 1-hour data collected at the lowest antenna elevation. Time series of the mean SNR is shown in Fig. 5. The gaps in the curves correspond to periods when data were not available.

The WSR-88D operates in two modes with the long and short radar transmit pulse. The brown line (Fig. 5) represents the pulse width: the upper part of the line corresponds to the long pulse and the lower part corresponds to the short pulse. As expected, the mean reflected power depends on the width of the radar pulse.

Fig. 5. Mean SNR_h from ground clutter (the blue line) from June to October 2015. WSR-88D KOUN. The brown line represents the pulse width. The higher line corresponds to the long radar pulse and the lower one represents the short pulse.

One can see that the mean SNR for the short pulse is about 3 to 4 dB lower than that for the long pulse. If homogenous scatterers like rain fill the radar resolution volume, this difference should be 9 dB. Because ground clutter is highly variable in range and is not exactly volumetric scatterers, this difference is smaller.

One can see that the mean SNR in the long pulse mode increased over time from 66.2 dB in June 2015 to 67.1 dB in September and October 2015. This could be due to a time change in vegetation, but one can expect some drop in the reflected power from more dry vegetation in October than in June. So this SNR growth is likely due to a system drift.

One can also see variations in SNR at a particular pulse width. For instance, a 4-dB drop in SNR on 13 June 2015 at about 6 UTC, 2.5-dB jumps on 30 June 2015, 2.5-dB oscillations on 19-25 July 2015 in the short pulse mode, 4-dB jump on 17 August 2015, and other.

The sharp variations in SNR could be caused by rain. Rain events are indicated in Fig. 6 with the green line. It is seen that the rain events correlate well with the drops of SNR. It is hard to imagine that rain in the vicinity of radar decreases reflections from the ground so these decreases are due to rain water on the radome. This can be recognized by using ground clutter and could be used to correct for attenuation caused by wet radome. The increases of SNR_h on 19 and 30 June 2015 (Fig. 6) are due to variations in radar parameters and should be monitored by the system. Fig. 7 shows the transmit powers measured by the KOUN's system hardware on 19 and 30 June 2015. One can see a drop in the horizontal power at about 06 UTC on 19 June 2015 whereas the SNR from ground clutter increases at that time. The gain of the H-receiver (not shown) did not change. So the increase of SNR from ground clutter on that day was not compensated by the system. Similar situation was observed on 30 June 2015. So SNR from the ground can be used to monitor short term system gain changes. We do not know if such short term variations are due to changes in the system gain or they are caused by the measurement processes in the radar or both. Further analysis is needed to resolve this issue.

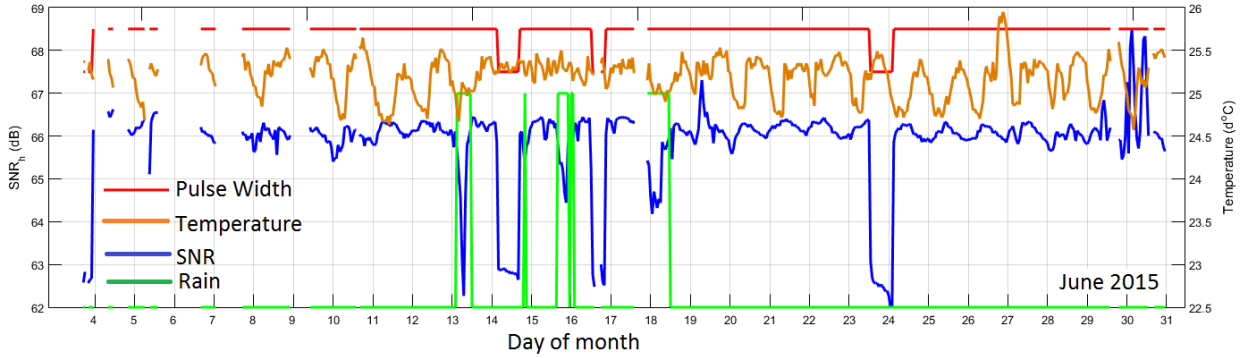

Fig. 6. Mean SNR_h from ground clutter (the blue line), the pulse width (red line), rain (green line), and AME temperature (brown line) in June 2015. WSR-88D KOUN.

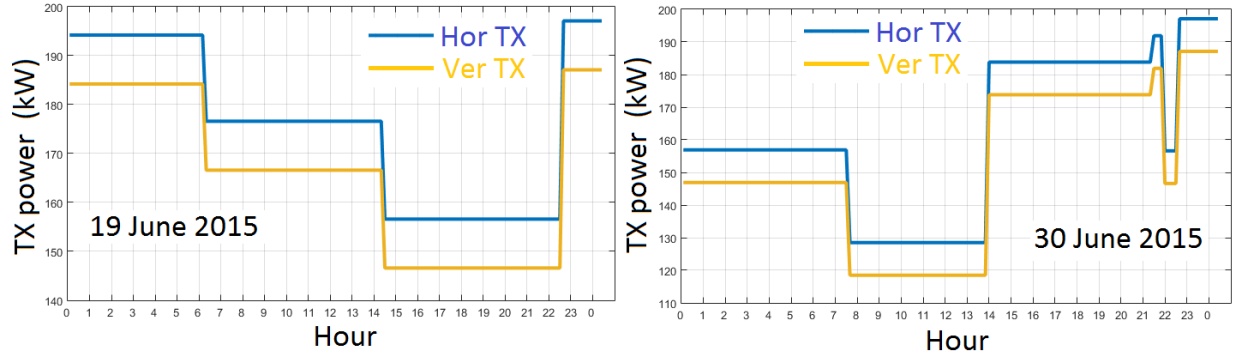

Fig. 7. The transmit powers in the horizontal (the blue line) and vertical (the light brown line) channels measured by the system on 19 and 30 June 2015. WSR-88D KOUN.

Variations in SNR from ground clutter caused by the temperature variations in the Antenna Mounted Electronics (AME) are about 0.5 dB, which is within the tolerable interval. The KOUN's data show that the system can be stable over time intervals of several hours to several days. So SNR_h from ground clutter can be used to monitor stability of reflectivity measurements if no rain is present within 30 km from radar, where ground clutter has been collected from.

5. Feasibility of Z_{DR} monitoring

The signal with the selected narrow spectra has been used to monitor the stability of Z_{DR} values measured in ground clutter. A time series of the measurements from June to October 2015 is presented in Fig. 8. Strong Z_{DR} peaks in the figure are observed during rain events on the KOUN site. It was shown in the previous section that rain decreases the mean SNR from ground clutter. Fig. 9 shows SNR_h and SNR_v from ground clutter on 13 June 2015 during rain. It is seen that SNR_h and SNR_v were about equal before and after rain and droped during rain, but the drop in SNR_v is larger than that in SNR_h. This means that rain attenuates radar signals in both channels, but attenuation in the vertical channel is stronger than that in the horizontal channel and that causes a positive jump in Z_{DR}. There is correlation between rain rate and SNR_h and SNR_v from the ground: signal attenuation in the channels increases with the increasing rain rate. Compare, for instance Fig. 9 and the lower panel in Fig. 10. But we do not see a strong (if any) correlation between the Z_{DR} jumps and the rain rate.

Positive jump in Z_{DR} in rain could have a contribution from ground clutter due to wet ground objects. To verify this, Z_{DR} from ground clutter was measured at times when rain was observed at ranges closer than 30 km from the radar but is not present yet at the radar site. The NRMN Oklahoma Mesonet station is located about 200 m to the west from KOUN so rain on the station can be considered as rain on KOUN site as well. The problem with this is that the Mesonet stations measure not rain rates but rain accumulations every 5 min, so the instantaneous rain rate is not available. The second issue is that radar data from the lowest elevation, where parameters of ground clutter are measured, are updated every 9 min in VCPs 31 and 32. So a time correspondence of the Mesonet and radar data is not precise. Figs. 10 present Z_{DR} from ground clutter averaged over one antenna sweep and the 5-min averaged rain rate from the NRMN Mesonet station. The figure shows weak correlation between Z_{DR} and the averaged rain rate: the strong rain rate maximum at about 0645 UTC does not correspond to a strong maximum in Z_{DR}; values of Z_{DR} are high from 0400 to 0830 UTC. Rain on the site began at about 0330 UTC.

On dry days, the stability of the mean Z_{DR} from the ground is mainly within ±0.1 dB (Fig. 8) and can be used to monitor system Z_{DR}. Note a significant difference in Z_{DR} variations in Figs. 8 and 10: this is due to averaging over 1 hour of data in Fig. 8.

It is seen in Fig. 8 that the mean Z_{DR} values from ground clutter are slightly different for the long and short pulses: in the short pulse mode, the mean Z_{DR} is about 0.1 dB lower than that in the long pulse mode. This should be taken into account in an operational monitoring of the system Z_{DR}.

No impacts of the wind, humidity, or temperature on the mean Z_{DR} from ground clutter have been noticed. An example is in Fig. 11, where Z_{DR} was not averaged over 1 hour and thus has larger variations than those in Fig. 8. More graphical results can be found in Melnikov and Zrnic (2015).

Sometimes variations in Z_{DR} from ground clutter have been observed in fair weather as in Fig. 12. Note a drop in Z_{DR} in panel (a) at 0000 – 0240 UTC and then its rebound to the mean value. The Z_{DR} values in the panel have not been averaged over 1 hour. Note also quite synchronous changes in SNR from ground clutter (panel b) except at the indicated time interval. Such variations should be tolerated by the system, i.e., some system parameters in the technical log should reflect such variations, and the system Z_{DR} should be adjusted automatically. The main technical system parameters for the day are shown in panels (c) and (d). Panel (c) presents the transmitted powers in the channels and panel (d) shows the Z_{DR} biases measured by the system. No variations that can be responsible for the Z_{DR} drop in panel (a) are seen. The technical parameters in panels (c) and (d) are quite stable at 0000-0400. Such events need to be analyzed further.

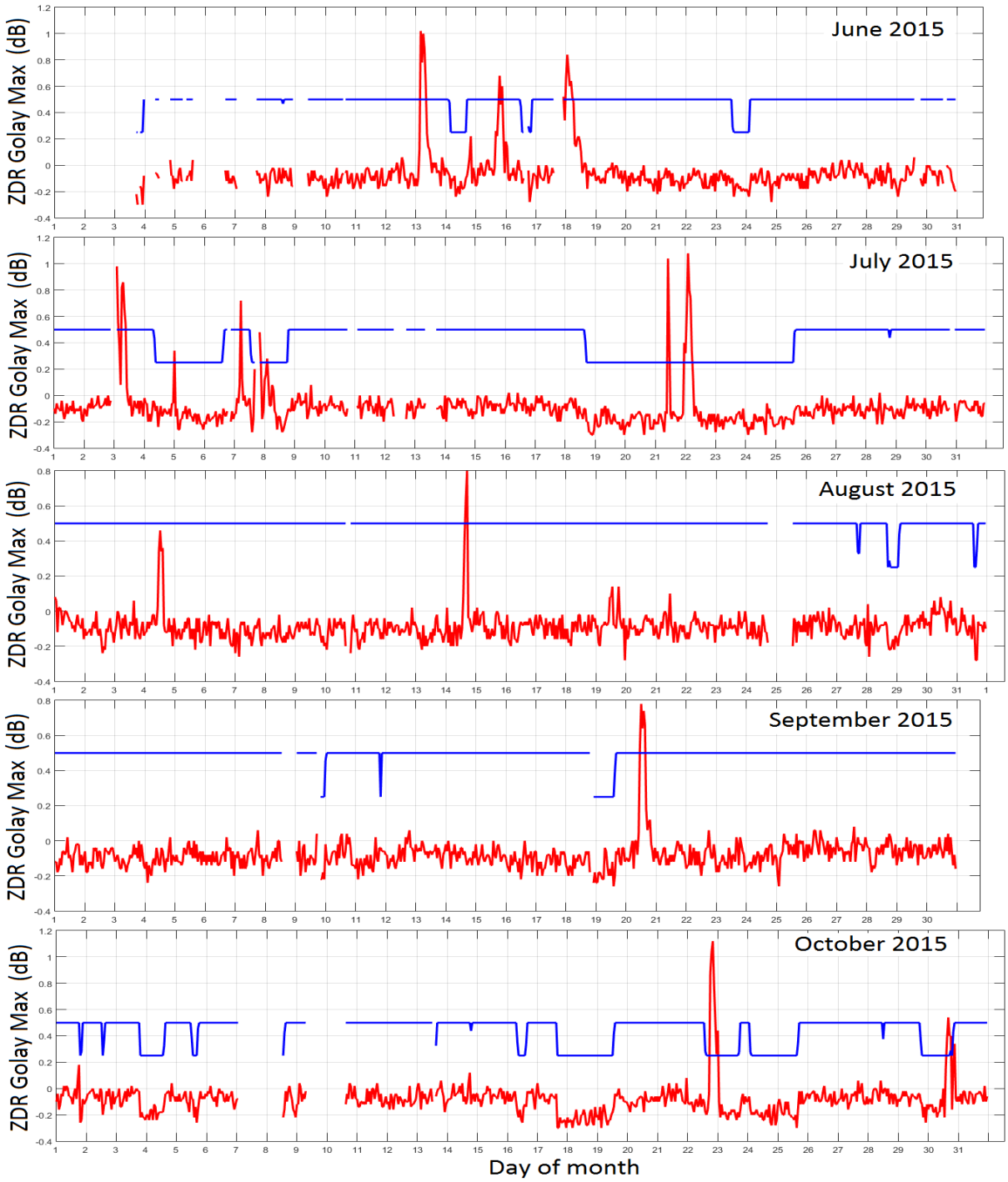

Fig. 8. Time series of the system Z_{DR} (the red lines) calculated using the Golay filter. The blue line represents the pulse width: values of 0.5 and 0.25 correspond to the long and short pulses. The curves brake at times when data are not available. WSR-88D KOUN, time is UTC.

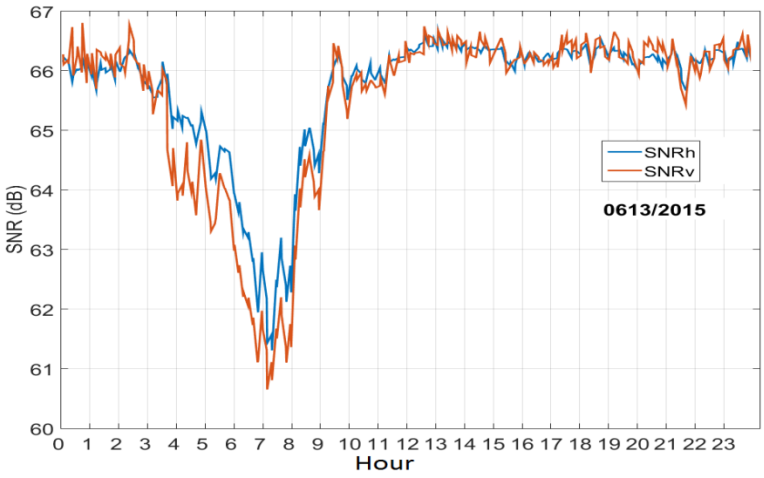

Fig. 9. SNR_h and SNR_v from ground clutter on 13 June 2015. Rain on the radar site occurred from about 0340 to 1145 UTC. See rain rates in Fig. 10.

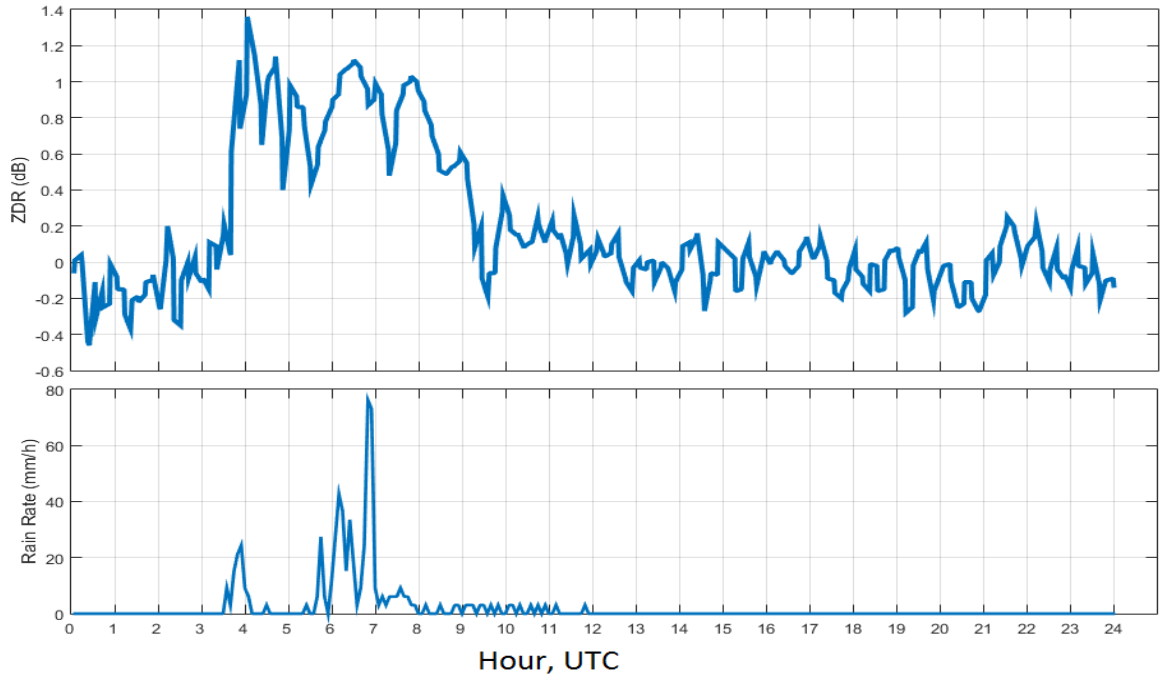

Fig. 10. (top): Z_{DR} at the distribution maximum obtained with the Golay filter on 13 June 2015. (bottom): Rain rate measured at the Oklahoma Mesonet station NRMN on the same day.

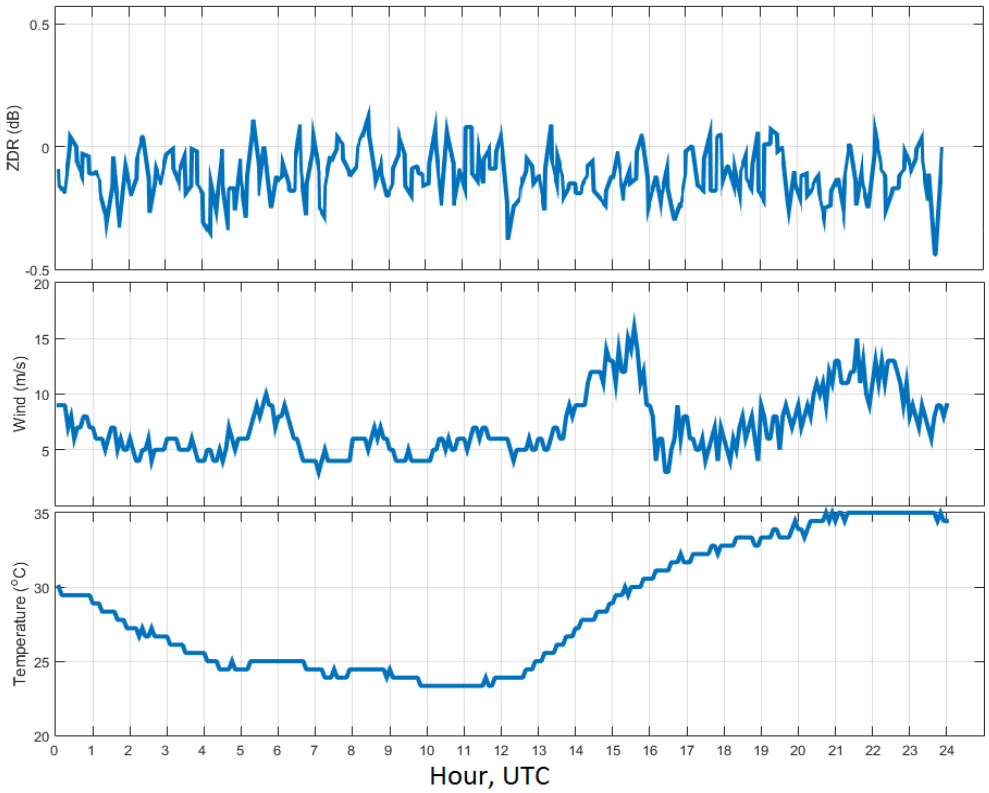

Fig. 11. Z_{DR} values of ground clutter (top panel), the wind velocity (central panel) and temperature (bottom panel) from Mesonet site NRMN at a height of 10 m on 5 August 2015.

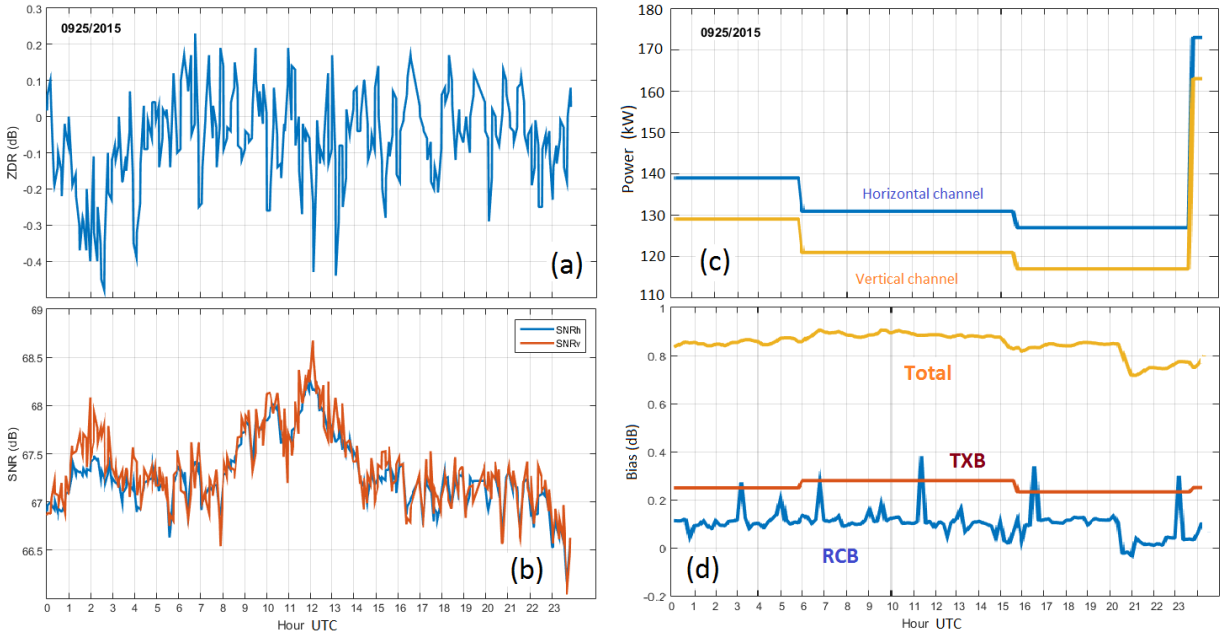

Fig. 12. (a): Z_{DR}, (b) SNR from ground clutter observed on 25 September 2015. The transmit powers and system Z_{DR} biases are in panels (c) and (d). WSR-88D KOUN.

6. Conclusions

Radar signal from the ground has been processed to establish its feasibility for monitoring stability of reflectivity and differential reflectivity measurements. The processing consists of the Fourier transformations of the signals, selecting a part of spectra located between -0.5 and +0.5 m s^{-1}, suppressing the rest of spectra, converting the spectra to voltages, and computing Z, $Z_{DR,}$ and SNR. It has been found that the mean SNR and the maximum of Z_{DR} distributions, averaged over 1 hour, can be used for monitoring the system stability. The mean SNR in the horizontal and vertical channels are within ±1 dB and Z_{DR} is within ±0.1 dB if the system is in a good technical stage and there is no rain within 30 km from radar. Such stability has been observed during time intervals from a few hours to several days.

The wind near the ground, humidity of the air, environmental temperature, and vegetation do not affect the Z_{DR} values measured in signals from the ground clutter. These measurements can be taken in the long and short pulse radar mode. In the short pulse mode, the mean Z_{DR} value in ground clutter is 0.1 dB lower than that measured in the long pulse mode. Temperature variations in the AME enclosure, where the receivers reside, of 0.5^{o}C lead to 0.5 dB variations in SNR and 0.1 dB variations in Z_{DR} measured from ground clutter. These variations leave SNR (reflectivity) and Z_{DR} inside tolerable changes.

Simultaneous measurements of Z_{DR} in ground clutter and in areas of Bragg scatter are consistently within 0.1 dB for the KOUN site. This also speaks for the feasibility of monitoring Z_{DR} by using ground clutter.

If rain is on the radar, Z_{DR} values from ground clutter increase. Rain water on the radome can decrease SNR from ground clutter by 5 dB and increase Z_{DR} by 1 dB. This should be studied further to assess the effect on the Z and Z_{DR} measurements and to compensate for these impacts.

Two unknowns in the studied procedure are:

- Very good agreement between the Z_{DR} values from ground clutter and from Bragg scatter is achieved on the WSR-88D KOUN located in central Oklahoma. For other radar sites with different orography, similar comparison should be obtained.
- The WSR-88Ds operate in a 300 MHz wide frequency band. The dependence of the measurements on the frequency in this band should be established. This can be done by comparing results obtained with KOUN (2705 MHz) and with practically collocated KCRI (2995 MHz).

These issues are not major obstacles for implementing the technique on the WSR-88D network. If there are dependences of Z_{DR} from ground clutter upon radar frequency and types of terrain, this difference is expected to be constant in time and can be taken into consideration in the monitoring of system stability.

Acknowledgments

We thank Mr. Scott Ganson for providing data about KOUN's system parameters. We are also thankful to the Oklahoma Mesonet staff for providing the data from the NRMN station.

References

Atlas, D. 2002: Radar Calibration: Some Simple Approaches. *Bull. Amer. Meteor. Soc.*, 83, 1313–1316.

Billingsley, J., 2002: Low Angle Radar Land Clutter: Measurements and Empirical Models. William Andrew, Inc., 703 pp.

Bringi, V. N., and V. Chandrasekar, 2001: *Polarimetric Doppler Weather Radar. Principles and Applications.* Cambridge University Press. 636 pp.

Borowska, L. and D. Zrnic, 2012: Use of Ground Clutter to Monitor Polarimetric Radar Calibration. *J. Atmos. Oceanic Technol.*, **29**, 159–176.

Cunningham, J.G., W. D. Zittel, R. Lee, and R. L. Ice, 2013: Methods for identifying systematic differential reflectivity (ZDR) biases on the operational WSR-88D network. 36th Conf. Radar Meteor. AMS, Breckenridge, CO. Online at: https://ams.confex.com/ams/36Radar/webprogram/Paper228792.html

Curtis, C. D., 2009: Exploring the capabilities of the agile beam phased array weather radar. Ph. D. Dissertation. University of Oklahoma, XXX pp.

Delrieu, G., S. Caoudal, and J. D. Creutin, 1997: Feasibility of using mountain return for the correction of ground-based X-band weather radar data. *J. Atmos. Oceanic Technol*., 14, 368–385.

Doviak, R.J., and D. S. Zrnic, 2006: *Doppler radar and weather observations*, 2nd ed., Academic Press, 2006. 562 pp.

Fabry, F., 2004: Meteorological value of ground target measurements by radar. *J. Atmos. Oceanic Technol.*, **21**, 560–573.

Frech, M., 2013: Monitoring the data quality of the new polarimetric weather radar network of the German Meteorological Service. 36th Conf. Radar Meteorol., Breckenridge, CO. Available online at: https://ams.confex.com/ams/36Radar/webprogram/Paper228472.html

Gorgucci, E., G. Scarchilli, and V. Chandrasekar, 1999: A procedure to calibrate multiparameter weather radar data using the properties of the rain medium. *IEEE Trans. Geosci. Remote Sens.*, **17**, 269–276.

Hoban, N.P., J. G. Cunningham, and D. Zittel, 2014: Estimating Systematic WSR-88D Differential Reflectivity (ZDR) Biases Using Bragg Scattering. *30th Conf. Environmental Information Processing Technologies.* AMS, Atlanta. Online at: https://ams.confex.com/ams/94Annual/webprogram/Paper237404.html

Hubbert J., M. Dixon, S. Ellis, and G. Meymaris, 2009: Weather radar ground clutter. Part I: Identification, modeling, and simulation. *J. Atmos. Oceanic Technol.*, 26, 1165–1180.

Ice, R.L., A. K. Heck, J. G. Cunningham and W. D. Zittel, 2014: Challenges of polarimetric weather radar calibration. ERAD 2014 - The Eighth European Conf. Radar Meteorol. Hydrology, Germany. Online at: http://www.pa.op.dlr.de/erad2014/programme/ExtendedAbstracts/117_Ice.pdf

Kulemin, G.P, 2003: *Millimeter-Wave Radar Targets and Clutter*. Artech House, 327 pp.

Lee, J-S., and E. Pottier, 2009: *Polarimetric Radar Imaging: from basics to application*. CRC Press, New York, 357 pp.

Long, M. W., 2001: *Radar Reflectivity of Land and Sea*. Artech House, 534 pp.

Melnikov, V., and D. Zrnic, 2004: Simultaneous Transmission Mode for the Polarimetric WSR-88D, NOAA/NSSL Report, 84 pp. Online at: http://www.nssl.noaa.gov/publications/wsr88d_reports

Melnikov, V.M., R. J. Doviak, D. S. Zrnic, and D. J. Stensrud**,** 2011: Mapping Bragg scatter with a polarimetric WSR-88D. *J. Atmos. Oceanic Technol.,* **28,** 1273-1285.

Melnikov, V., D. Zrnic, M. Schmidt, and R. Murnan, 2013: Z_{DR} calibration issues in the WSR-88Ds. NSSL interim report, 54 pp. Online: http://www.nssl.noaa.gov/publications/wsr88d_reports/WSR88D_ZDRcalib_Report_2013.pdf

Melnikov, V., and D. Zrnic, 2015. Feasibility of monitoring ZDR calibration using ground clutter. NSSL interim report, 35 pp. Available online at: http://www.nssl.noaa.gov/publications/wsr88d_reports/NPI_2015_report.pdf

Meneghini, R., and T. Kozu, 1990: *Spaceborn Weather Radar*. Artech House, 197 pp.

Middleton, D., 1960: *Statistical Communication Theory*. McGrawHill, 1140 pp.

Pellarin, T., G. Delrieu, and J. D. Creutin, 1999: Variability of mountain returns during dry-weather conditions: Applications to radar calibration control. Preprints, 29th Conf. on Radar Meteorology, Montreal, QC, Canada, Amer. Meteor. Soc., 772–775.

Rinehart, R. E., 1978: On the use of ground return targets for radar reflectivity factor calibration checks. *J. Appl. Meteor.*, **17**, 1342–1350.

Schaffner, M., P. L. Smith, K. R. Hardy, and K. M. Glover, 1975: Comments on ‘‘Applications of radar to meteorological operations and research.’’ *Proc. IEEE*, **63**, 731–733.

Sugier, J., and P. Tabary, 2006: Evaluation of dual polarization technology at C-band for operational weather radars as part of the EUMETNET OPERA program. 4th European Conf. Radar Meteorol. Hydrolog., Barcelona, Spain. Available online at: http://www.crahi.upc.edu/ERAD2006/proceedingsMask/00010.pdf

Vaisala Co., 2014: Meteorological Solutions Worldwide. http://www.vaisala.com/en/meteorology/products/weatherradars/Pages/default.aspx

Vukovic, Z.R., J. M. C. Young, and N. Donaldson, 2015: An operational use of ground clutter to monitor radar performance. 37th Conf. Radar Meteorol. AMS, Norman, OK. Available online at: https://ams.confex.com/ams/37RADAR/webprogram/Paper275669.html

Williams, E., K. Hood, D. Smalley, M. Donovan, V. Melnikov, D. Forsyth, D. Zrnic, D. Burgess, M. Douglas, J. Sandifer, D. Saxion, O. Boydstun, A. Heck, and T. Webster, 2013: End-to-end calibration of Nexrad differential reflectivity with metal spheres. 36th Conf. Radar Meteor. AMS, Breckenridge, CO. Online at: https://ams.confex.com/ams/36Radar/webprogram/Paper228796.html

Wallace, P.R., 1953: Interpretation of the fluctuating echo from randomly distributed scatterers. *Can J. Physics*, **31**, 995-1009.

Zhang, J., K. Howard, C. Langston, S. Vasiloff, B. Kaney, A. Arthur, S. Van Cooten, K. Kelleher, D. Kitzmiller, F. Ding, D-J. Seo, E. Wells, C. Dempsey, 2011: National Mosaic and Multi-Sensor QPE (NMQ) System: Description, Results, and Future Plans. Bull. Amer. Meteor. Soc., 92, 1321-1338.

Zrnic, D., V. Melnikov and A. Ryzhkov, 2006a: Correlation coefficients between horizontally and vertically polarized returns from ground clutter. *J. Atmos. Oceanic Technol.*, **23**, 381–394.

Zrnic D.S., V. M. Melnikov, and J. K. Carter, 2006b: Calibrating differential reflectivity on the WSR-88D. *J. Atmos. Ocean. Technol*., **23**, 944-951.